The cell wall polymer lipoteichoic acid becomes non-essential in *Staphylococcus aureus* cells lacking the ClpX chaperone

Kristoffer T. Bæk[a#], Lisa Bowman[b], Charlotte Millership[b], Mia Dupont Søgaard[a], Volkhard Kaever[c], Pia Siljamäki[d,e], Kirsi Savijoki[d] Pekka Varmanen[d], Tuula A. Nyman[e], Angelika Gründling[b] and Dorte Frees[a#]

Department of Veterinary Disease Biology, Faculty of Health and Medical Sciences, University of Copenhagen, Frederiksberg, Denmark[a]; Section of Microbiology and MRC Centre for Molecular Bacteriology and Infection, Imperial College London, London, United Kingdom[b]; Research Core Unit Metabolomics, Hannover Medical School, Hannover, Germany[c]; Department of Food and Environmental Sciences, University of Helsinki, Finland[d]; Institute of Biotechnology, Proteomics Unit, University of Helsinki, Finland[e]

Running head: Lack of ClpX bypasses LTA essentiality in *S. aureus*

#Address correspondence to Dorte Frees, df@sund.ku.dk, or Kristoffer T Bæk, ktb@sund.ku.dk.

Word count: 181 (abstract); 5,593 (body)

20 **Abstract**

21 Lipoteichoic acid (LTA) is an important cell wall component of Gram-positive bacteria
22 and a promising target for the development of vaccines and antimicrobial compounds
23 against *Staphylococcus aureus*. Here we demonstrate that mutations in the conditional
24 essential *ltaS* (LTA synthase) gene arise spontaneously in an *S. aureus* mutant lacking
25 the ClpX chaperone. A wide variety of *ltaS* mutations were selected and among these a
26 substantial part resulted in premature stop-codons and other changes predicted to
27 abolish LtaS synthesis. Consistent with this assumption, the *clpX ltaS* double mutants
28 did not produce LTA, and genetic analyses confirmed that LTA becomes non-essential
29 in the absence of the ClpX chaperone. In fact, inactivation of *ltaS* alleviated the severe
30 growth defect conferred by the *clpX* deletion. Microscopic analyses showed that the
31 absence of ClpX partly alleviates the septum placement defects of an LTA depleted
32 strain, while other phenotypes typical of LTA-negative *S. aureus* mutants including
33 increased cell size and decreased autolytic activity are retained. In conclusion, our
34 results indicate that LTA has an essential role in septum placement that can be
35 bypassed by inactivating the ClpX chaperone.

36 **Importance**

37 Lipoteichoic acid is an essential component of the *Staphylococcus aureus* cell
38 envelope, and an attractive target for the development of vaccines and antimicrobials
39 directed against antibiotic resistant Gram-positive bacteria such as methicillin resistant
40 *S. aureus* and vancomycin resistant *Enterococci*. In this study we show that the
41 lipoteichoic acid polymer is only essential for growth of *S. aureus* as long as the ClpX
42 chaperone is present in the cell. Our results indicate that lipoteichoic acid and ClpX play
43 opposite roles in a pathway that controls two key cell division processes in *S. aureus*,
44 namely septum formation and autolytic activity. The discovery of a novel functional
45 connection in the genetic network that controls cell division in *S. aureus* may expand the
46 repertoire of possible strategies to identify compounds or compound combinations that
47 kill antibiotic resistant *S. aureus*.

48 **Introduction**

49 *Staphylococcus aureus* remains a leading cause of hospital- and community-acquired
50 skin and soft tissue infections as well as of life-threatening invasive diseases (1). While
51 β-lactams like penicillin and methicillin were once effective antibiotics in treating
52 staphylococcal infections, the spread of methicillin-resistant *S. aureus* (MRSA) has
53 made treatment increasingly difficult (2). The profound ability of *S. aureus* to acquire
54 resistance towards clinically relevant antibiotics has prompted an interest in identifying
55 targets that can be used for the development of novel antibiotics with activity against
56 MRSA (3).

57 The cell wall polymer lipoteichoic acid (LTA) has been proposed as an attractive target
58 for the development of both vaccines and antimicrobial compounds directed against *S.*
59 *aureus* (reviewed in Reference 4). LTA is found abundantly in the cell wall of many
60 gram-positive bacteria and is defined as an alditolphosphate-containing polymer that is
61 attached to the outside of the cytoplasmic membrane via a lipid anchor (4). Gram-
62 positive bacteria synthesize different types of LTA that, based on their chemical
63 structures, are grouped into different types (4, 5). *S. aureus*, like many other Firmicutes,
64 produces type I LTA consisting of an unbranched 1-3 linked glycerolphosphate (GroP)
65 backbone chain. The addition of GroP residues to the tip of the growing LTA-chain
66 takes place at the outer surface of bacterial membranes, and is catalyzed by the LTA
67 synthase (LtaS) enzyme (6). The exact cellular function of LTA remains unknown, but
68 importantly LTA is essential for growth of *S. aureus* under standard laboratory growth
69 conditions (6, 7). Depletion of LtaS results in cell enlargement, aberrant positioning of
70 division septa, and ultimately cell lysis, pointing to a functional link between LTA and the

71 cell division process (6, 8). Consistent with this idea, LtaS of *S. aureus* was recently
72 shown to interact with numerous early and late cell-division proteins as well as enzymes
73 involved in peptidoglycan synthesis (9). In the rod-shaped Firmicutes *Bacillus subtilis*
74 and *Listeria monocytogenes*, inactivation of LTA synthesis also interferes with cell
75 division which is evident by cell filamentation and delocalization of the FtsZ cell division
76 initiator protein (10, 11). A functional link between LTA synthesis and cell division
77 therefore seems to be conserved within the family of Firmicutes. Other observations,
78 however, indicate that the essential role of LTA in *S. aureus* is, at least partly, related to
79 osmoprotection. First, LTA-deficient *S. aureus* strains can be propagated under
80 osmotically stabilizing conditions (8). Secondly, growth of an *S. aureus ltaS* mutant is
81 rescued by inactivation of GdpP, a phosphodiesterase that hydrolyzes the essential
82 signaling molecule cyclic-di-AMP, which is implicated in the control of potassium
83 transport, an important ion in osmotic homeostasis (7, 8). In fact, type I LTA was
84 recently proposed to share functionality with the osmoregulated periplasmic glucans
85 (OPG) that accumulate in the periplasm of gram-negative bacteria under low-osmolarity
86 conditions (4).

87 The highly conserved ClpX chaperone has a dual role in the cell, as it both targets
88 proteins for degradation by associating with the ClpP peptidase, and independently of
89 ClpP, facilitates protein folding and interactions (12). In *S. aureus*, inactivation of *clpX*
90 severely reduced virulence in both localized and systemic models of infections
91 suggesting that ClpX is indispensable for *S. aureus* pathogenesis (13, 14). Consistent
92 with this observation, ClpX controls, by an unknown mechanism, the transcription of a
93 number of major virulence genes, and the translation of Protein A and the global

94 virulence regulator, Rot (14–16). ClpX belongs to the Hsp100 family of heat shock
95 proteins that become critical during heat stress and other stresses conferring protein
96 folding stress (12). Surprisingly, inactivation of *clpX* in *S. aureus* improved survival at
97 high temperatures indicating that ClpX does not function as a classical heat shock
98 chaperone in this bacterium (14). Consistent with this notion, *clpX* transcription is not
99 inducible by heat stress in *S. aureus* (14). Inactivation of ClpX in *S. aureus* did,
100 however, severely impair growth at 30°C and below (14). The molecular mechanism
101 underlying this phenotype is unknown, and is not shared by a mutant lacking ClpP,
102 suggesting that it is the ClpP-independent chaperone activity of ClpX that is important
103 for growth of *S. aureus* at 30°C (14). In the present study we used a whole genome
104 sequencing approach to characterize compensatory mutations that arise spontaneously
105 with high frequency when the *clpX* deletion mutant is propagated at 30°C and below.
106 Intriguingly, the most frequent type of detected mutations was loss-of-function mutations
107 in the *ltaS* gene. Essentiality of LtaS in the isogenic wild-type strains was confirmed,
108 thus demonstrating that *S. aureus* can grow without LTA in the absence of the ClpX
109 chaperone. To gain insight into the mechanisms underlying the requirement for LTA, a
110 phenotypic characterization of the *clpX ltaS* double mutant was performed. From this
111 analysis we conclude that disruption of *clpX* compensates for the absence of LTA by a
112 c-di-AMP independent pathway that appears to be linked to cell division.

113 **Results**

114 **Inactivation of ClpX confers a severe growth defect at 30°C that is independent of**
115 **the strain background and of ClpP**

116 Previously we reported that an *S. aureus clpX* mutant forms colonies of very reduced
117 size at 30°C (14). The original *clpX* mutant was constructed in the laboratory *S. aureus*
118 strain 8325-4 that has very low activity of the SigB stress-response regulator (14, 17).
119 We therefore first set out to assess if the cold-sensitive phenotype of the *clpX* mutant is
120 conserved in SigB proficient *S. aureus* strains. The effect on growth of a *clpX* deletion
121 was examined in more detail in four different backgrounds namely the widely used
122 laboratory strains 8325-4 and Newman, the low-passage clinical isolate SA564, and
123 JE2, an erythromycin sensitive derivative of the community acquired MRSA strain,
124 USA300 LAC. In all strain backgrounds, the *clpX* deletion mutants formed colonies that
125 were slightly smaller than wild-type colonies at 37°C or temperatures above (Fig. 1A
126 and data not shown). When the temperature was reduced to 30°C or 25°C, the *clpX*
127 mutants formed barely visible colonies demonstrating that deletion of *clpX* confers a
128 growth defect to *S. aureus* that increase with decreasing temperatures in all strain
129 backgrounds (Fig. 1A and data not shown). Introduction of a *clpX* complementing
130 plasmid enables the *clpX* mutant strain to form colonies of wild-type size (Fig. 1B).
131 Growth assays in liquid medium at 30°C showed that the *clpX* mutants exhibited 42 -
132 67% lower exponential growth rates (depending on strain background; Fig. 1C), and
133 that the *clpX* mutant reached a much lower final density (CFUs per ml or OD; Fig. 1D
134 and 1E) independently of the size and growth status of the inoculum (Fig. S1). At 37°C
135 the growth defect of the *clpX* mutants was much less severe, as the cultures reached

136 roughly the same final CFUs per ml as the respective wild type strains and the
137 exponential growth rates were only slightly reduced (14 - 25%; Fig. 1C and 1D).

138 ClpX can associate with ClpP to form the ClpXP protease. To investigate if ClpX
139 contributes to growth at low temperatures via a ClpP dependent pathway, we examined
140 the effect of a *clpP* deletion on growth. We found that although the *clpP* mutants grew
141 slower than the parental strains, similar reductions in exponential growth rates were
142 observed at 30°C (27 - 29%) and 37°C (22 - 33%; Fig. 1C). Additionally, the
143 temperature had little effect on endpoint CFUs per ml (Fig. 1D). Thus, the growth defect
144 conferred by the *clpP* deletion does not mimick the temperature-dependent effect of the
145 *clpX* deletion, suggesting that it is the ClpP-independent chaperone activity which is
146 required for growth at temperatures below the optimum. The ClpC chaperone is an
147 alternative substrate recognition factor for ClpP, and to rule out that the impaired growth
148 of the *clpX* mutant is caused by an abnormal activity of ClpCP (due to the absence of
149 ClpX), we constructed an *S. aureus* 8325-4 *clpX clpP* double mutant (KB1506) and
150 compared its growth with the 8325-4 *clpX* single mutant. As seen in Fig. 1E the *clpX*
151 *clpP* double mutant exhibited a growth defect similar to that of the *clpX* mutant,
152 supporting the notion that the *clpX* growth phenotype is not mediated via ClpCP. In
153 summary, inactivation of the ClpX chaperone activity in *S. aureus* confers a cold
154 sensitive phenotype to *S. aureus* that is independent of ClpP and of the strain
155 background.

156 **Loss-of-function mutations in the *ltaS* gene arise spontaneously in *clpX* mutants**
157 **grown at temperatures below optimum**

158 When the *clpX* mutant strains are plated at 30°C, larger colonies consistently appear
159 among the very small colonies (Fig. 2A), indicating that the growth defect associated
160 with lack of ClpX can be alleviated genetically by the acquisition of spontaneous
161 suppressor mutations. The frequency of large suppressor colonies in cultures of the
162 *clpX* mutants after 24 h of growth at 30°C was 0.12 ± 0.06 in the 8325-4 *clpX*
163 background, and 0.92 ± 0.04 in the SA564 *clpX* background. One suspected suppressor
164 mutant, strain 564-25-2, with restored growth at 30°C (Fig. 1A and 2B) was chosen for
165 Illumina genome sequencing. The sequencing analysis revealed that strain 564-25-2
166 deviated from the parental SA564 *clpX* strain by only one single nucleotide
167 polymorphism (SNP) located in the *ltaS* gene and causing a H476Q substitution in the
168 lipoteichoic acid (LTA) synthase enzyme, LtaS. Interestingly, the H476 residue was
169 previously found to be essential for LtaS activity (18). To examine if mutations in *ltaS*
170 were common among the *clpX* suppressor colonies, the *ltaS* gene was sequenced in a
171 number of the suppressor mutants. The suppressor mutants were selected either
172 directly on solid media without a culturing step, or by passaging independent cultures of
173 the 8325-4 *clpX* strain at 30°C until large suppressor colonies accounted for at least
174 90% of the CFU count (details are described in Materials and Methods). Remarkably,
175 mutations in *ltaS* were identified in seven of the ten independent 8325-4 *clpX* cultures
176 as well as in a large number of the remaining suppressor strains selected in both the
177 8325-4 and SA564 strain backgrounds. As depicted in Fig 3A, these mutations resulted
178 in premature stop-codons, amino acid substitutions, and in-frame deletions.

179 The *ltaS* mutations were predicted to be loss-of-function mutations based on the
180 selection of a mutation changing the essential histidine at position 476 to a glutamine,
181 and the frequent selection of mutations resulting in premature stop-codons (18).
182 Consistent with this prediction, the LTA polymer was absent from the two representative
183 strains 83-25C ($LtaS_{382STOP}$ isolated in the 8325-4 *clpX* background) and 564-25-2
184 ($LtaS_{H476Q}$; Fig. 3B). The LTA immunoblot showed a stronger LTA signal in the 8325-4
185 *clpX* mutant, indicating that ClpX impacts LTA expression; however, this difference was
186 not reproducible (data not shown) consistent with our experience that LTA immunoblots
187 should be interpreted qualitatively rather than quantitatively. LtaS expression was not
188 altered by inactivation of either *clpX* or *clpP* but a strong LtaS band was detected in
189 strain 564-25-2 confirming previous results (18) that the non-functional $LtaS_{H476Q}$ variant
190 is expressed in higher amounts than the wild-type LtaS (Fig 3B and Table S3).

191 The loss-of-function mutation in *ltaS* was the only genetic change introduced in the
192 genome sequenced 564-25-2 suppressor mutant, strongly suggesting that inactivation
193 of LtaS results in the improved growth of the *clpX* mutant. In support hereof, the growth
194 defect of the SA564 *clpX* strain was restored to a similar extent by disrupting the *ltaS*
195 gene with an *ltaS::erm* marked deletion introduced by phage transduction (Fig 3C). We
196 conclude therefore that inactivation of the conditionally essential LtaS synthase
197 alleviates the growth defect caused by inactivation of the ClpX chaperone.

198 **LTA becomes non-essential in cells devoid of ClpX chaperone activity**

199 LTA has been reported to be essential for growth of *S. aureus* at 37°C. Therefore we
200 were surprised to find that the two *clpX* suppressor-mutants confirmed to harbor loss-of-

201 function mutations in *ltaS* improved growth of the *clpX* mutant not only at 30°C but also
202 at 37°C; the *clpX ltaS* double mutants were, however, not capable at growing at 44°C
203 (Fig. 1A). The finding that the LTA-negative suppressor mutants grow well at 37°C
204 indicates that LTA becomes non-essential in *S. aureus* cells lacking ClpX. To verify this,
205 we performed a genetic linkage analysis to test whether the wild-type *clpX* allele
206 (marked by inserting the *ermB* gene in a nearby non-coding sequence (19)) can be
207 back-transduced into the *clpX ltaS* suppressor mutant. As shown in Table 1, the wild-
208 type *clpX* gene was not co-transduced along with *ermB* into the LTA-negative *clpX*
209 strains, whereas we obtained a high frequency of co-transduction when using LTA-
210 positive *clpX* mutant strains as recipients. This result is highly significant ($p < 0.0005$)
211 indicating that LTA is indeed essential under the conditions used in this study, and that
212 LtaS becomes non-essential in the absence of the ClpX chaperone. To confirm this
213 result, plasmid pKB1469 expressing ClpX under the control of an anhydrotetracycline
214 (AHT) inducible promoter was introduced into strain 83-25C. As predicted, this strain
215 lost viability upon induction of ClpX expression at 37°C showing that LtaS is essential in
216 a ClpX-positive strain (Fig. 3D). In contrast, no effect on viability was observed when
217 expression of ClpX was induced at 30°C (Fig.3D) which is in line with the finding by Oku
218 et al. (8) that LtaS is non-essential at 30°C.

219 **Inactivation of ClpX compensates for the absence of LTA by a novel c-di-AMP**
220 **independent pathway**

221 An *S. aureus gdpP* mutant can, similarly to a *clpX* mutant, grow without LTA (7). The
222 GdpP phosphodiesterase cleaves the second messenger c-di-AMP, and consequently
223 the intracellular concentration of c-di-AMP is significantly increased in *gdpP* mutant

224 strain (7). Interestingly, the *S. aureus clpX* mutant shares some phenotypes with a *gdpP*
225 mutant, namely a decrease in cell size, a small increase in peptidoglycan cross-linking
226 (7, 19), and as shown here, the ability to grow without LTA. To assess if these shared
227 phenotypes correlated with increased intracellular c-di-AMP levels in the *clpX* mutant,
228 we quantified c-di-AMP levels in cytoplasmic extracts from cultures of strains SA564
229 and JE2, the corresponding *clpX* mutant strains, and the suppressor strain 564-25-2
230 (*ltaS clpX*) using an LC-MS/MS method (7). The results (Fig. 4) showed no significant
231 differences in cellular levels of c-di-AMP between the wild types and the mutant strains,
232 suggesting that inactivation of *clpX* bypasses the requirement for LTA by a c-di-AMP
233 independent pathway.

234 **Lack of ClpX improves septum formation in LTA depleted cells**

235 Depletion of LtaS in *S. aureus* confers a number of distinct phenotypes including
236 morphological changes such as an increase in cell size, misplacement of division septa,
237 and a tendency to clump (6). Similar changes were reported when an RN4220 *ltaS*
238 mutant was grown under conditions permissive for growth (8). Inactivation of *clpX* on
239 the other hand did not impact septum localization but resulted in significantly smaller
240 cells with a thickened cell wall (19). The finding that LtaS becomes non-essential in a
241 *clpX* mutant strain, prompted us to investigate if the absence of the ClpX chaperone
242 counteracted some of the morphological phenotypes of LtaS depleted cells. Light and
243 transmission electron microscopy (TEM) of the wild type, the *clpX* single mutant, and
244 the *clpX ltaS* double mutant grown at 30°C or 37°C showed that the majority of the *clpX*
245 *ltaS* double mutant cells exhibit wild-type placement of the division septa, that is,

246 septum formation that occurs at the mid-cell and mostly perpendicular to previous
247 division planes (Fig. 5A, 5B and S2). The *clpX ltaS* cells were, however, larger and
248 more irregularly shaped than wild-type cells or *clpX* single mutant cells, and additionally
249 the cell wall was thicker, more irregular, and had a fuzzier appearance (Fig 5B). To
250 directly investigate the effect on cell division of depleting LTA in cells that lack *clpX*, *S.*
251 *aureus* strains with IPTG inducible *ltaS* expression were created in either an 8325-4
252 wild-type (8325-4-*iltaS*) or an 8325-4 *clpX* (8325-4-*clpX*-*iltaS*) genetic background. As
253 expected, in the absence of IPTG and hence *ltaS* expression, cells with an intact *clpX*
254 gene stopped growing whereas cells with a disrupted *clpX* gene were able to continue
255 growth, corroborating the above conclusion that LTA becomes non-essential when ClpX
256 is inactivated (Fig. S3). Extensive cell wall synthesis at the division site was observed in
257 the presence of LTA both in the presence and absence of an intact *clpX* gene (Fig. 5A,
258 S4 and S5). Depletion of LTA also resulted in cell enlargement regardless of *clpX* status
259 (Fig. 5A, S4, and S5). However, while LTA depletion led to a reduction in visible septum
260 formation in the wild-type background, septum formation was still prevalent after LTA
261 depletion in the *clpX* background (Fig. 5A, S6, and S7). In summary, inactivation of
262 *clpX* appears to rescue the reduced ability of LTA deficient cells to lay down the septum
263 correctly, whereas lack of *clpX* does not counteract other phenotypes associated with
264 the lack of LTA: namely a larger cell size, thicker and more irregular cell wall, and cell
265 clustering.

266 **Inactivation of LtaS decreases peptidoglycan crosslinking and increases**
267 **susceptibility to vancomycin and cefoxitin**

268 Inactivation of *clpX* causes a small increase in peptidoglycan cross-linking and
269 decreases susceptibility to several types of antibiotics targeting the cell wall, and we,
270 hence, speculated that the cellular changes underlying these phenotypes might be
271 correlated to the ability of the *clpX* mutant to tolerate LTA deficiency (19). To examine
272 the changes in cell wall properties in more detail we compared the muropeptide profiles
273 of SA564 wild-type, *clpX*, and *clpX ltaS* mutant cells. This analysis revealed that while
274 the peptidoglycan profiles from SA564 wild-type and *clpX* mutant cells are very similar,
275 the peptidoglycan from the LTA deficient *clpX ltaS* mutant was characterized by a
276 severe reduction in highly cross-linked muropeptides (>8-mers), and a concomitant
277 increase in the relative fraction of dimers to octamers (Fig 5C). Next, we determined the
278 susceptibilities of the strains towards antibiotics targeting the cell envelope. This
279 analysis revealed that the *clpX ltaS* double mutant is more sensitive towards cefoxitin
280 and vancomycin than the *clpX* mutant and the wild-type strains, and slightly more
281 sensitive to oxacillin (Table 2). In contrast, the *ltaS* mutation did not affect susceptibility
282 towards imipenem and ertapenem that both belong to the carbapenem class of β-
283 lactams. As shown previously (19), the *clpX* deletion had only minor effects on the
284 susceptibility to oxacillin and daptomycin in the strains SA564 and 8325-4, and no effect
285 on susceptibility to cefoxitin and vancomycin. Taken together, these results indicate that
286 the introduction of loss-of-function mutations in *ltaS* concomitantly decrease
287 peptidoglycan cross-linking and susceptibility to some cell wall targeting antibiotics. The
288 effect of the *clpX* and *ltaS* mutations varied greatly with the type of antibiotic, and there

289 was no trend supporting that the cellular changes responsible for decreasing antibiotic
290 susceptibility of the *clpX* mutant are contributing to the ability of the *clpX* mutant to grow
291 in the absence of LTA.

292 **The LTA and ClpX have opposite roles in determining the level of surface-bound**
293 **autolysins**

294 LTA is critical for maintaining normal levels of peptidoglycan hydrolase activity, and
295 binding of the major *S. aureus* autolysin, Atl, to the cell wall seems to involve direct
296 interactions between Atl and LTA (20). We therefore examined autolytic activity of our
297 strains and found that the autolytic activity of the *clpX ltaS* double mutant was greatly
298 reduced in a Triton X-100 autolysis assay, demonstrating that the *clpX ltaS* double
299 mutant, similar to LTA depleted cells, has reduced autolytic activity (Fig. 6A). To follow
300 up on this finding, a zymographic analysis was performed. In the zymographic analysis
301 the activity of the major autolysin, Atl, is visible in multiple bands reflecting that Atl is a
302 bifunctional murein hydrolase that is produced as a 138-kDa precursor protein,
303 sequentially cleaved to generate 115- and 85-kDa intermediate products, and further
304 processed to generate a 62-kDa N-acetylmuramyl-L-alanine amidase (AM) and a 51-
305 kDa N-acetylglucosaminidase (GL; Fig. 6B). Consistent with the Triton-X-autolysis
306 assay, the zymographic profile of cell extracts derived from the *clpX ltaS* double mutant
307 demonstrated that the intensity of Atl bands was reduced in the *clpX ltaS* double
308 mutant, when compared to the profiles of wild-type, or *clpX* mutant cells. The only
309 exception is the band originating from the 62-kDa mature AM that has the same
310 intensity as in wild-type extracts. In contrast, inactivation of *clpX* alone increased the
311 intensity of this band and an 85-kDa variant of Atl (Fig. 6B). In the zymographic

312 analysis, activity of the Sle1 autolysin is also clearly visible. As previously reported, the
313 level of Sle1 is a substrate of ClpXP and consequently present at elevated levels in *clpX*
314 and *clpP* mutant cells (21). Strikingly, the level of Sle1, similar to the 62-kDa mature
315 AM, was again reduced to wild-type levels in the *clpX ltaS* double mutant.

316 *S. aureus* encodes a number of additional enzymes predicted to possess autolytic
317 activity, but their activity is not visible in the zymographic analysis. In order to
318 investigate the general impact of ClpX and LTA on the levels of autolytic enzymes
319 bound to the cell surface, the surface proteome ("surfacome") was analyzed by trypsin
320 shaving followed by MS identification. The surfacome analyses identified two other
321 predicted autolysins, SceD and Aaa, in addition to Atl that were identified with the
322 highest identification scores in the surfacome of the single *clpX* mutant strain (Table
323 S2), suggesting that the three autolysins are expressed at higher levels, or that their
324 stability is increased at the cell surface of the *clpX* mutant compared to the wild-type or
325 the *clpX ltaS* strains. This confirms that ClpX has a negative impact on the level of Atl
326 and two other surface bound autolysins. The comparable identification scores of these
327 three autolysins shaved from wild-type and *clpX ltaS* double mutant cells further
328 supports that inactivation of LtaS in cells lacking ClpX reduces the amount of these
329 surface-bound autolysins back to wild-type levels. Taken together, our results suggest
330 that LTA and ClpX have opposite roles in determining the level of several surface-bound
331 autolysins.

332 **Discussion**

333 LTA is an abundant cell wall polymer that has attracted interest as a novel antibacterial
334 target owing to its essential role for growth of *S. aureus* (22). Moreover, LTA seems to
335 have an important role in resistance to β-lactams, as MRSA strains can be re-sensitized
336 to some β-lactams by reducing expression of the *ltaS* gene (23). Thus, compounds
337 targeting LTA synthesis may have the additional advantage that they can be used in
338 combination with β-lactams to effectively combat MRSA.

339 The exact role of LTA remains unknown, and the pleiotropic phenotypes associated with
340 depletion of LTA have represented a challenge for dissecting why LTA is conditional
341 essential for growth of *S. aureus*. In the present study we show that mutations
342 abolishing the function of LtaS arise spontaneously in an *S. aureus* mutant lacking the
343 ClpX chaperone. The finding that the combined deletion of the *ltaS* and *clpX* genes
344 results in cells that grow almost as well as wild-type cells, despite that each of the single
345 deletions confers a severe growth defect to *S. aureus* cells, indicates that ClpX and LTA
346 have opposite roles in a pathway that is critical for growth of *S. aureus*. The effect of
347 deleting either the *clpX* or the *ltaS* gene is strongly dependent on temperature: deletion
348 of *clpX* impairs growth severely at 30°C and mildly at 37°C and, vice versa, deletion of
349 *ltaS* results in loss of viability at 37°C but for some strains not at 30°C.

350 Phenotypic analysis revealed that the *clpX ltaS* double mutant retained most of the
351 hallmark phenotypes associated with LTA depletion including morphological changes
352 such as enlarged cell size, a thickened, irregular cell wall, and impaired cell separation
353 following cell division. The latter phenotype has been explained by the substantially
354 reduced autolytic activity in cells lacking LTA (8). Interestingly, here we showed that a

355 number of autolysins including the major autolysin Atl are more abundant in the
356 surfacome of *S. aureus* cells lacking ClpX, and that the level of autolysins are reduced
357 to wild-type level or lower by the subsequent inactivation of LtaS. Taken together our
358 results show that LTA and ClpX have opposite roles in determining the level of surface-
359 bound autolysins. Hence, one possible scenario is that the dual inactivation of ClpX and
360 LtaS may help to balance the aberrant autolytic activity caused by the single inactivation
361 of either ClpX or LtaS. However, the validity of this hypothesis is questioned by our
362 finding that the *clpX ltaS* double mutant, despite the near wild-type expression of Atl and
363 other autolysins, retained phenotypes associated with reduced expression of autolysins
364 such as a deficiency in cell separation and very low autolytic activity in a Triton-X-100
365 autolysis assay.

366 LTA depletion is also characterized by reduced cell wall synthesis at the septum and
367 aberrant positioning of division septa (7, 8). Intriguingly, we showed here that in LTA
368 depleted cells that lack a functional *clpX* gene, extensive septum formation was
369 observed at mid-cell suggesting that inactivation of *clpX* to some extent alleviates the
370 septum-placement defects associated with LTA deficiency. The partly restored septum
371 formation in cells lacking both ClpX and LTA implies that cell division is central in
372 understanding the functional link between ClpX and LTA activity. In almost all bacteria,
373 cell division is orchestrated by the tubulin homologue, FtsZ, which polymerizes to form a
374 ring-like structure, the Z-ring that establishes the location of the division site (24). The Z-
375 ring is tethered to the cell membrane by the essential FtsA protein that also has a role in
376 the formation of larger FtsZ bundles, as well as for recruiting downstream cell division
377 proteins (24). It has been found that the ClpX chaperone modulates FtsZ polymer

378 dynamics in bacteria as diverse as *Escherichia coli*, *B. subtilis*, and *Mycobacterium*
379 *tubercolosis* suggesting that ClpX has a widely conserved role in cell division by
380 interacting directly with FtsZ (25–27). Similarly, several observations indicate that LtaS
381 also has a direct role in cell division. First, LtaS accumulates at the division site where it
382 has been proposed to be part of a large multi-enzyme complex containing early stage
383 division proteins like FtsA, as well as late stage cell division proteins (9). Additionally, *S.*
384 *aureus* cells depleted for both LTA and WTA lose the ability to establish the Z-ring (28).
385 The literature therefore supports the scenario that both LTA and ClpX have a direct role
386 in cell division. Our finding that the combined inactivation of LtaS and ClpX abolished
387 the growth-defect conferred by each of the single mutations suggests that ClpX and
388 LTA have antagonistic roles in the cell division process of *S. aureus*.

389

390 In conclusion, we have shown that the LTA cell wall polymer becomes non-essential for
391 growth of *S. aureus* if cells are devoid of ClpX chaperone activity by a novel c-di-AMP
392 independent pathway. The presented data indicate that ClpX and LTA have opposing
393 roles in the coordination of two key cell division processes *S. aureus* namely septum
394 formation and control of autolytic activity thereby providing novel insight into the function
395 of this important cell wall polymer of Gram-positive bacteria.

396 **Materials and Methods**

397 **Bacterial strains and growth conditions**

398 Strains used in this study are listed in Table S1. Strain constructions are described in
399 Supplementary Materials and Methods (Text S1). *E. coli* strains were cultured in Luria
400 broth (LB) at 37°C or 30°C, or on LB medium solidified with 1.5% w/v agar. *S. aureus*
401 strains were cultured in tryptic soy broth (TSB) at 37°C or 30°C with aeration, or on TSB
402 medium solidified with 1.5% w/v agar (TSA). When inoculating *clpX* deletion strains,
403 care was taken to avoid visibly larger colonies containing potential suppressor mutants.
404 *S. aureus* JE2-derived strains were obtained from the Network of Antimicrobial
405 Resistance in Staphylococcus aureus (NARSA) program (supported under NIAID/NIH
406 contract HHSN272200700055C).

407

408 **Growth curves and growth rate calculations**

409 Growth of *S. aureus* strains was assessed by measuring optical density (OD_{600}) of
410 cultures grown in Erlenmeyer flasks or in a Bioscreen C instrument (Oy Growth Curves
411 Ab Ltd, Finland), and by determining the number of CFUs per ml in cultures grown in
412 Erlenmeyer flasks. Overnight cultures were grown in TSB at 37°C. For growth curves in
413 Erlenmeyer flasks, overnight cultures were diluted 1:200 in 30 ml TSB giving a starting
414 OD_{600} of approx. 0.015 - 0.03, and incubated with aeration at 30°C or 37°C with or
415 without antibiotics as indicated. OD_{600} values were determined at 1 h intervals and
416 CFUs per ml culture were determined at 2h intervals by performing serial dilutions in

417 0.9% w/v NaCl and plating 100 µl on TSB plates. Plates were then incubated at 37°C
418 and colonies were enumerated after overnight growth. The colony size distribution in
419 *clpX* cultures was clearly bimodal allowing easy distinction between small and larger
420 presumed suppressor colonies. For growth in the Bioscreen C instrument overnight
421 cultures were diluted in 300 µl TSB to an OD_{600} of approx. 0.001, and OD_{600} was
422 measured every 5 min with 20 seconds of shaking before each measurement.

423 All exponential growth rates were determined by growing the relevant strains in a
424 Bioscreen C instrument as described above. The growth rates were automatically
425 calculated by applying a custom R script (29) using a linear regression function kindly
426 provided by the Botstein laboratory
427 (http://www.princeton.edu/genomics/botstein/protocols/Growth-Rate-Using-R.pdf). In
428 short, OD_{600} values were log-transformed and linear regressions were determined for
429 each data point in the OD_{600} interval from 0.02 to 0.12 based on a window containing 15
430 data points. The exponential growth rate was identified as the maximal slope of the
431 linear regressions. The script for calculation of growth rates was validated on simulated
432 growth data obtained from the logistic growth equation for growth yield as a function of
433 time (t), growth rate (µ), and lag time (30). The standard deviation was calculated using
434 values from different biological replicates. Statistical significance was calculated using
435 Student's t-test. Doubling time in minutes was calculated as $\ln 2/\mu \times 60$.

436

437

438 **Genetic suppressor analysis**

439 SA564 and 8325-4 *clpX* mutants were streaked for single colonies on tryptic soy agar
440 plates and incubated at 37°C overnight. Several small colonies were then resuspended
441 in 0.9% (w/v) NaCl and dilutions were spread on TSA plates that were incubated at
442 25°C, 30°C or 37°C. Colonies that appeared visibly larger than the background colonies
443 were colony purified twice and stored. In addition, ten independent overnight cultures of
444 8325-4 *clpX* grown at 37° were diluted 1:1000 into 1 ml fresh TSB medium, and
445 incubated with aeration at 30°C. After 24 hours, the cultures were transferred again to
446 fresh medium by a 1:1000 dilution. Each day bacteria were plated on TSA at 30°C to
447 determine the proportion of large suppressor colonies. After two passages at 30°C, all
448 cultures contained at least 90% suppressors, and one large colony from each culture
449 was purified and stored. The *ltaS* gene was amplified by PCR with primers KB71F and
450 KB71R on genomic DNA prepared from 26 suppressor mutants isolated in the SA564
451 and 8325-4 backgrounds, and sequenced by capillary sequencing using primers
452 KB71F, KB73F and KB71R.

453 **Co-transduction experiment**

454 KB1241 was used as donor for bacteriophage Φ11 transduction into strains 8325-
455 4Δ*clpX*, 83-25C and KB1262, or bacteriophage Φ85 transduction into strains
456 SA564Δ*clpX* and 564-25-2, selecting for erythromycin (5 mg/l) resistance. The presence
457 of the *ermB* gene was confirmed in the transductants by PCR with the primers KB76F
458 and KB76R (19) prior to testing for co-transduction of the wild-type *clpX* allele by PCR

459 with the primers saclpx385f and saclpx2447r (14). Statistical significance was calculated
460 using Pearson's Chi-squared test.

461 **SNP detection**

462 One of the obtained suppressor mutants in the SA564 *clpX* genetic background (564-
463 25-2) was chosen for SNP detection. Genomic DNA was prepared from overnight
464 cultures of the SA564 *clpX* strain and the suppressor strain 564-25-2 grown in TSB at
465 37°C, and sequenced on an Illumina Hi-Seq 2000 instrument (Fasteris, SA, Geneva,
466 Switzerland). The sequencing reads obtained by Illumina sequencing of SA564 *clpX*
467 and the suppressor mutant 564-25-2 were aligned to the assembled SA564 genome
468 (GenBank accession numbers CP010890 and CP010891 for chromosome and plasmid,
469 respectively; Reference 31) using Bowtie2 (version 2.2.3, default parameters;
470 Reference 32). The sequences have been submitted to the European Nucleotide
471 Archive under accession number PRJEB8687. Alignments were converted to sorted,
472 indexed binary alignment map (BAM) files, and SNPs and indels were called with
473 SAMtools and BCFtools (version 1.1, default parameters; Reference 33). Using
474 BEDtools (version 2.21.0; Reference 34) the average read coverage was calculated to
475 695 for strain 564-25-2 and 410 for strain SA564 Δ*clpX*. The sequencing reads from
476 SA564 *clpX* or 564-25-2 covered the whole reference genome except for the expected
477 *clpX* deletion in both strains (position 2066206 to 2066840) and a 14-nt deletion in an
478 intergenic region (position 2273962 to 2273975) in both strains. The SA564 reference
479 genome was annotated with the RAST server (35), and annotations and calculated
480 amino acid changes were assigned to the variant set using a custom R script. Variants
481 were excluded if the quality score for the base call was <100, or if the phred-scaled *p*-

482 value using Fisher's exact test for strand bias was >200 for indels or >60 for SNPs. The
483 filtered variants were verified by capillary sequencing using appropriate PCR primers
484 (Table S2). By this method, one SNP (A2274642T) in the tRNA-Leu-CAA gene was
485 identified between the reference genome and our SA564 wild type, no SNPs were
486 identified between the SA564 wild type and the SA564 *clpX* mutant, and one SNP
487 (C1082972A) in the *ltaS* gene ($LtaS_{H476Q}$) was identified between strain 564-25-2 and
488 the SA564 *clpX* mutant.

489

490 **LtaS depletion and fluorescence microscopy**

491 *S. aureus* strains 8325-4, 8325-4-Δ*clpX*, and 8325-4-Δ*clpXltaS*$_{stop}$ were grown overnight
492 at 37°C in TSB. Strains 8325-4-*iltaS* and 8325-4Δ*clpX-iltaS* were grown in TSB with
493 erythromycin 10 µg/ml and 1 mM isopropyl β-d-thiogalactosidase (IPTG). The following
494 day, bacteria from a 1 ml culture aliquot were harvested and washed three times with
495 1 ml TSB. Next, 6 ml TSB (substituted where necessary with 1 mM IPTG) was
496 inoculated with 60 µl washed bacterial suspensions (1:100 dilution) and cultures
497 incubated at 37°C with shaking. The OD_{600} values were recorded every two hours for 8
498 hours. To maintain the culture in log phase, at the 4 h time point the cultures were again
499 back diluted 1:100 into 5 ml fresh TSB (when required substituted with 1 mM IPTG) and
500 growth continued for an additional 4 hours. The average OD_{600} values and standard
501 deviations from three independent experiments were plotted. At the 4 h time point, 1 ml
502 of culture was removed and prepared for the detection of LTA by western blot.

503 For microscopy, strains were grown as described above with the exception that strain
504 NCTC8325-4-*iltaS* propagated in the absence of IPTG was diluted 1:10 at the 4 h point,
505 to obtain sufficient material for the subsequent microscopy analysis. At the 7 h time
506 point, bacteria from a 2 ml of culture were harvested by centrifugation for 2 minutes at
507 17,000 x g. Cells were washed 3 times with PBS pH 7.4. The cells were suspended in a
508 volume of PBS to give a final OD_{600} of 3. Coverslips were prepared in advance by
509 coating them with 100 μl of a 0.1% polylysine solution and washing 4 times with PBS pH
510 7.4. Next, 100 μl of cells were placed on the coverslip for 3 minutes and washed 3 times
511 with PBS. Finally, 100 μl of a 1 μg/ml vancomycin-BODIPY (Molecular Probes) solution
512 was added to the immobilized bacteria and incubated for 5 to 20 minutes and
513 subsequently washed 3 times with PBS. The coverslips were mounted onto a slide
514 containing 20 μl of Vectashield (Vector Laboratories). Cells were visualized on a Zeiss
515 Axio Imager A2, using a GFP filter and images were captured with an AxioCam MRc
516 Rev.3 camera.

517

518 **Electron microscopy**

519 Overnight cultures grown at 37°C were diluted 1:200 into 40 ml of fresh TSB and grown
520 at 30°C or 37°C to an OD_{600} of 0.5. Bacteria from a 10-ml culture aliquot were collected
521 by centrifugation at 8,000 x g, and the cell pellets were suspended in fixation solution
522 (2.5% glutaraldehyde in 0.1 M cacodylate buffer [pH 7.4]; Electron Microscopy
523 Sciences, PA) and incubated overnight at 4°C. The fixed cells were further treated with
524 2% osmium tetroxide, followed by 0.25% uranyl acetate for contrast enhancement. The

525 pellets were dehydrated in increasing concentrations of ethanol, followed by pure
526 propylene oxide, and then embedded in Epon resin. Thin sections for electron
527 microscopy were stained with lead citrate and observed in a Philips CM100 BioTWIN
528 transmission electron micro- scope fitted with an Olympus Veleta camera with a
529 resolution of 2,048 by 2,048 pixels. Sample processing and microscopy were performed
530 at the Center for Integrated Microscopy, Faculty of Health and Medical Sciences,
531 University of Copenhagen.

532

533 **Peptidoglycan analysis**

534 One (for the wild type and the 564-25-2 mutant) or two liters (for the *clpX* mutant) of
535 TSB medium was inoculated with overnight cultures of *S. aureus* strains SA564,
536 SA564Δ*clpX* and strain 564-25-2, to an OD_{600} of 0.06 and grown at 30°C to late-log
537 phase (OD approximately 1.6 for the wild type and strain 564-25-2, and 0.8 for the *clpX*
538 strain). The cultures were cooled on ice and the bacteria were subsequently collected
539 by centrifugation. Peptidoglycan was purified, digested with mutanolysin, and analyzed
540 by high-performance liquid chromatography (HPLC), as described previously (7).
541 Muropeptide profiles were determined for each strain in duplicate, and HPLC
542 chromatograms from one representative experiment are shown. Data analysis was
543 carried out as described previously (19).

544

Acknowledgements

We thank Annette Garbe for her help with c-di-AMP mass spectrometry.

548 **Table 1: Number of transductants harboring either the wild-type or the Δ*clpX***

549 **allele when using different *S. aureus* recipient strains**

	Phage transduction recipient				
Co-transduction of wt *clpX* allele[1]	8325-4 *clpX*	8325-4 *clpX* *ltaS*$_{382STOP}$	8325-4 *clpX* *ltaS*$_{W122STOP}$	SA564 *clpX*	SA564 *clpX* *ltaS*$_{H476Q}$
Yes	13	0	0	12	0
No	3	12	11	2	10

550 [1]Replacement of the Δ*clpX* allele with the wild-type allele was assessed by PCR.

551 **Table 2: MICs (mg/L) for different antibiotics of *clpX* and *clpX ltaS* mutants in**

552 **SA564 and 8325-4**

	8325-4			SA564		
Antibiotic	WT	*clpX*	*clpX* *ltaS*$_{382*}$	wt	*clpX*	*clpX* *ltaS*$_{H476Q}$
Oxacillin	0.19-0.25	0.38 - 0.5	0.094	0.38-0.5	1.5 - 4	0.25
Imipenem	0.047	0.047	0.032	0.064	0.064	0.023
Ertapenem	0.19	0.19	0.094	0.19	0.25	0.19
Cefoxitin	3	3	0.38	4	4	1
Daptomycin	0.38-0.75	0.75 - 1	0.38	0.25	0.38	0.38
Vancomycin	1.5	1.5	0.25	1.5	1	0.19

553

554 **Figure legends**

555 **Fig 1: ClpX is required for growth at low temperatures in *S. aureus*.**

556 **A.** ClpX is required for growth at low but not high temperatures. The wild-type *S. aureus*
557 strain SA564 and the indicated derivatives were grown in TSB at 37°C. At OD_{600} = 0.5,
558 the cultures were diluted 10^1, 10^2, 10^3 and 10^4-fold, and 5 µL of each dilution was
559 spotted on TSA plates that were subsequently incubated at the indicated temperatures.
560 **B.** The *clpX*-related growth defect can be complemented. The wild-type *S. aureus* strain
561 SA564 and the corresponding *clpX* mutant harboring either a plasmid expressing ClpX
562 under an anhydrotetracycline (AHT)-inducible promoter (pKB1469), or the empty vector,
563 were grown in TSB at 37°C and diluted 10^1, 10^2, 10^3, 10^4 and 10^5-fold. Five µL of each
564 dilution was spotted on TSA plates containing 25 ng/ml AHT that were subsequently
565 incubated at 30°C. **C.**.Growth rates of wild-type and mutant strains at 30°C and 37°C.
566 Cultures of SA564, JE2, or Newman strains and their corresponding *clpX* and *clpP*
567 mutants were grown overnight at 37°C, diluted into 300 µl TSB, and growth was
568 measured at 30°C in a Bioscreen C instrument. Values represent mean specific growth
569 rates (h^{-1}) +/- the standard deviation of at least three biological replicates. Numbers
570 above each bar indicate mean doubling time in minutes. Statistically significant
571 differences between each mutant and the wild types, or between the two mutants (as
572 indicated by the horizontal bar) are indicated with asterisks (* $p < 0.05$; ** $p < 0.001$). **D**.
573 Final CFU/ml yield at 30°C and 37°C. Overnight cultures of SA564 and the indicated
574 mutant strains were diluted 1:200 in TSB and grown at the indicated temperature for 24
575 h. Cultures were diluted, plated and incubated at 37°C. Values represent mean CFU/ml

576 +/- the standard deviation of at least three biological replicates. Statistically significant
577 differences between each mutant and the wild type, or between the two mutants (as
578 indicated by the horizontal bar) are indicated with asterisks (* $p < 0.05$; ** $p < 0.001$). **E**.
579 Growth curve of *clpX clpP* double mutant. *S. aureus* strain 8325-4 and corresponding
580 *clpX, clpP,* and *clpX clpP* strains were grown overnight at 37°C, and diluted into 300 µl
581 TSB, and growth was measured at 30°C in a Bioscreen C instrument. Values represent
582 mean OD readings +/- the standard deviation (error bars are smaller than the symbol
583 size) of three biological replicates.

584 **Fig 2: Spontaneous suppressor mutants restore growth of the *S. aureus clpX***
585 **mutant**

586 **A.** Faster growing suppressor mutants appear spontaneously in *clpX* cultures grown at
587 low temperature. An overnight culture of the *S. aureus* SA564 *clpX* mutant was grown at
588 30°C in TSB, diluted and spread on a TSA plate, and incubated at 30°C for 48 hours. **B.**
589 Growth of the *S. aureus* SA564 wild-type strain, the SA564 *clpX* strain, and the
590 spontaneous suppressor strain 564-25-2 ($ltaS_{H476Q}$) at 30°C in TSB measured as
591 CFU/ml. Colony formation was assessed by incubating plates for 48 hours at 30°C.
592 '*clpX* small' indicate the count of small, normal-sized, colonies, and '*clpX* large' indicate
593 the count of large suppressor colonies. Values represent mean of three replicates, and
594 error bars indicate standard deviation.

595 **Fig 3: Mutations in the *ltaS* gene restore growth of the *S. aureus clpX* mutant**

596 **A.** Topology map of LtaS showing the location and class of the identified suppressor
597 mutations. **B.** Analysis of LTA synthesis. Extracts obtained from *S. aureus* strains

598 SA564 wild-type, SA564 *clpX*, SA564 *clpP*, 564-25-2 (SA564 *clpX ltaS*$_{H476Q}$), 8325-4
599 wild-type, 8325-4 *clpX*, and 83-25C (*clpX ltaS*$_{382STOP}$) grown at 30°C and normalized
600 based on optical density (OD_{600}) readings of the original cultures were separated by
601 SDS/PAGE, electrotransferred to a PVDF membrane, and subjected to immunoblotting
602 using an LTA-specific or an LtaS-specific antibody as indicated. **C.** Growth of the *S.*
603 *aureus* SA564 wild-type strain, the SA564 *clpX* strain, the spontaneous suppressor
604 strain 564-25-2 (SA564 *clpX ltaS*$_{H476Q}$), and the SA564 *clpX ltaS*::*erm* strain at 30°C in
605 TSB. **D.** LtaS is essential at 37°C but not at 30°C. The 8325-4 *clpX ltaS*$_{382STOP}$
606 suppressor mutant harboring either a plasmid expressing ClpX under an AHT-inducible
607 promoter, or the empty vector, were grown in TSB at 37°C and diluted 10^1, 10^2, 10^3 and
608 10^4-fold. 10 µL of each dilution was spotted on TSA plates supplemented with AHT as
609 indicated and subsequently incubated at either 30°C or 37°C.

610 **Fig 4: Cyclic-di-AMP levels in *S. aureus* are not affected by inactivation of *clpX* or**
611 ***clpP*.**

612 Intracellular c-di-AMP concentration. The concentration of c-di-AMP in the cytoplasm of
613 the indicated strains were determined by LC-MS/MS. Values indicate c-di-AMP/mg
614 bacterial dry weight, and the average and standard deviation of three replicates are
615 plotted.

616 **Fig 5: Cell morphology, septum formation and cell wall structure is affected by**
617 **inactivation of *clpX* and by the compensatory loss of LtaS activity.**

618 **A.** Fluorescence microscopic analysis of wild-type, *clpX* inactivated, and LTA depleted
619 strains. *S. aureus* strain 8325-4 and its corresponding *clpX*, and *clpX-ltaS*$_{STOP}$ mutants
620 were grown in TSB to exponential phase at 37°C. Strains 8325-4 *iltaS* and 8325-4 *clpX-*
621 *iltaS* were grown to exponential phase at 37°C in the presence of 1 mM IPTG, then
622 diluted into medium with or without 1 mM IPTG and grown for 3 h at 37°C. Bacteria
623 were stained with BODIPY-vancomycin and prepared for fluorescence microscopy as
624 described in materials and methods. Examples of raw microscope images can be seen
625 in Fig. S4-S7. **B.** TEM analysis of wild-type, *clpX* inactivated, and LTA-negative strains.
626 The SA564 wild type, the SA564 *clpX* strain, and the 564-25-2 (SA564 *clpX ltaS*$_{H476Q}$)
627 strain were grown in TSB to log-phase at 37°C, and prepared for electron microscopy
628 as described in materials and methods. **C.** Peptidoglycan structure in SA564 wild type,
629 the SA564 *clpX* strain, and the 564-25-2 (SA564 *clpX ltaS*$_{H476Q}$) strain. HPLC
630 chromatograms of mutanolysin digested peptidoglycan purified from the indicated
631 strains, and percentages indicating the relative abundance of monomers, dimers,
632 trimers to 8-mers, and higher oligomers, respectively in each strain. Representative
633 results of two individual experiments are shown.

634 **Fig 6: An LTA-negative strain has decreased autolytic activity**

635 **A.** Autolysis assay. *S. aureus* strain SA564 and the corresponding *clpX*, *clpP* and *clpX*
636 *ltaS*$_{H476Q}$ mutants were analyzed for autolytic activity using a Triton X-100 autolysis
637 assay. **B**. Zymogram assay. SA564 and its derived strains were grown to exponential

638 phase, and equal amounts of cell wall-associated proteins from were loaded onto an
639 SDS polyacrylamide gel containing heat-killed *S. aureus* SA564 wild-type cells.
640 Representative results of three independent experiments are shown. The positions of
641 the molecular mass standards are indicated on the left (in kilodaltons). Atl and Sle1
642 protein levels were quantified relative to the wild-type strain using ImageJ.

643

644 **Supplementary figure legends:**

645 **Fig. S1**. Effect of size and growth phase of inoculum on growth of *clpX* mutant. *S.*
646 *aureus* strains 8325-4 and 8325-4 *clpX* were grown to exponential (OD ~0.1; "exp") or
647 stationary (overnight culture; "stat") phase at 37°C, diluted as indicated (1:10 or 1:1000)
648 into 300 µl TSB, and growth was measured at 30°C in a Bioscreen C instrument. Values
649 represent mean OD readings +/- the standard deviation (error bars are smaller than the
650 symbol size) of three biological replicates.

651 **Fig. S2**. Microscopic analysis of wild type, *clpX* inactivated, and LTA-negative strains.
652 *S. aureus* SA564 wild type, the SA564 *clpX* strain, and the 564-25-2 (SA564 *clpX*
653 $ltaS_{H476Q}$) strain were grown in TSB to log-phase at either 30°C or 37°C, samples were
654 prepared for microscopy analysis, and bacteria stained with BODIPY-vancomycin. Left
655 panels show phase contrast images, right panels show fluorescence images.

656 **Fig. S3. A.** Growth curves of *S. aureus* 8325-4 and derived strains. Overnight cultures
657 of *S. aureus* strains 8325-4 (WT), 8325-4-Δ*clpX*, 8325-4-Δ*clpX* $ltaS_{stop}$, 8325-4-*iltaS*
658 (WT-*iltaS*) and 8325-4Δ*clpX-iltaS* were harvested, washed, and diluted 1:1000 into TSB
659 substituted with 1 mM IPTG. Cultures were incubated at 37°C, and OD_{600} values were
660 recorded. To maintain the cultures in log phase, at the 4 h time point the cultures were
661 back diluted 1:100 into 5 ml fresh TSB (when required substituted with 1 mM IPTG) and
662 growth continued for an additional 4 hours. The average OD_{600} values and standard
663 deviations from three independent experiments are plotted. **B.** Analysis of LTA
664 synthesis. Extracts obtained from *S. aureus* strains 8325-4 (WT), 8325-4-Δ*clpX*, 8325-4-
665 Δ*clpX* $ltaS_{stop}$, 8325-4-*iltaS* (WT-*iltaS*) and 8325-4Δ*clpX-iltaS* were separated by

666 SDS/PAGE, electrotransferred to a PVDF membrane, and subjected to immunoblotting
667 using an LTA-specific antibody.

668 **Fig. S4.** Fluorescence microscopic analysis of strain 8325-4 *iltaS* grown to exponential
669 phase at 37°C in the presence of 1 mM IPTG, and stained with BODIPY-vancomycin.
670 Bacteria were grown and prepared for fluorescence microscopy as described in
671 materials and methods.

672 **Fig. S5.** Fluorescence microscopic analysis of strain 8325-4 *clpX iltaS* grown to
673 exponential phase at 37°C in the presence of 1 mM IPTG, and stained with BODIPY-
674 vancomycin. Bacteria were grown and prepared for fluorescence microscopy as
675 described in materials and methods.

676 **Fig. S6.** Fluorescence microscopic analysis of strain 8325-4 *iltaS* grown to exponential
677 phase at 37°C in the absence of IPTG, and stained with BODIPY-vancomycin. Bacteria
678 were grown and prepared for fluorescence microscopy as described in materials and
679 methods.

680 **Fig. S7.** Fluorescence microscopic analysis of strain 8325-4 *clpX iltaS* grown to
681 exponential phase at 37°C in the absence of IPTG, and stained with BODIPY-
682 vancomycin. Bacteria were grown and prepared for fluorescence microscopy as
683 described in materials and methods.

684

685

686

687 **References**

688 1. **Lowy FD**. 1998. *Staphylococcus aureus* infections. N Engl J Med **339**:520–532.

689 2. **DeLeo FR**, **Otto M**, **Kreiswirth BN**, **Chambers HF**. 2010. Community-associated
690 meticillin-resistant *Staphylococcus aureus*. Lancet **375**:1557–1568.

691 3. **Richter SG**, **Elli D**, **Kim HK**, **Hendrickx APA**, **Sorg JA**, **Schneewind O**, **Missiakas**
692 **D**. 2013. Small molecule inhibitor of lipoteichoic acid synthesis is an antibiotic for Gram-
693 positive bacteria. Proc Natl Acad Sci USA **110**:3531–3536.

694 4. **Percy MG**, **Gründling A**. 2014. Lipoteichoic acid synthesis and function in gram-
695 positive bacteria. Annu Rev Microbiol **68**:81–100.

696 5. **Schneewind O**, **Missiakas D**. 2014. Lipoteichoic acids, phosphate-containing
697 polymers in the envelope of gram-positive bacteria. J Bacteriol **196**:1133–1142.

698 6. **Gründling A**, **Schneewind O**. 2007. Synthesis of glycerol phosphate lipoteichoic
699 acid in *Staphylococcus aureus*. Proc Natl Acad Sci USA **104**:8478–8483.

700 7. **Corrigan RM**, **Abbott JC**, **Burhenne H**, **Kaever V**, **Gründling A**. 2011. c-di-AMP is
701 a new second messenger in *Staphylococcus aureus* with a role in controlling cell size
702 and envelope stress. PLoS Pathog **7**:e1002217.

703 8. **Oku Y**, **Kurokawa K**, **Matsuo M**, **Yamada S**, **Lee B-L**, **Sekimizu K**. 2009. Pleiotropic
704 roles of polyglycerolphosphate synthase of lipoteichoic acid in growth of *Staphylococcus*
705 *aureus* cells. J Bacteriol **191**:141–151.

706 9. **Reichmann NT**, **Piçarra Cassona C**, **Monteiro JM**, **Bottomley AL**, **Corrigan RM**,
707 **Foster SJ**, **Pinho MG**, **Gründling A**. 2014. Differential localization of LTA synthesis

708 proteins and their interaction with the cell division machinery in *Staphylococcus aureus*.
709 Mol Microbiol **92**:273–286.

710 10. **Schirner K**, **Marles-Wright J**, **Lewis RJ**, **Errington J**. 2009. Distinct and essential
711 morphogenic functions for wall- and lipo-teichoic acids in *Bacillus subtilis*. EMBO J
712 **28**:830–842.

713 11. **Webb AJ**, **Karatsa-Dodgson M**, **Gründling A**. 2009. Two-enzyme systems for
714 glycolipid and polyglycerolphosphate lipoteichoic acid synthesis in Listeria
715 monocytogenes. Mol Microbiol **74**:299–314.

716 12. **Kirstein J**, **Hoffmann A**, **Lilie H**, **Schmidt R**, **Rübsamen-Waigmann H**, **Brötz-**
717 **Oesterhelt H**, **Mogk A**, **Turgay K**. 2009. The antibiotic ADEP reprogrammes ClpP,
718 switching it from a regulated to an uncontrolled protease. EMBO Mol Med **1**:37–49.

719 13. **Farrand AJ**, **Reniere ML**, **Ingmer H**, **Frees D**, **Skaar EP**. 2013. Regulation of host
720 hemoglobin binding by the *Staphylococcus aureus* Clp proteolytic system. J Bacteriol
721 **195**:5041–5050.

722 14. **Frees D**, **Qazi S**, **Hill PJ**, **Ingmer H**. 2003. Alternative roles of ClpX and ClpP in
723 *Staphylococcus aureus* stress tolerance and virulence. Mol Microbiol **48**:1565–1578.

724 15. **Frees D**, **Sørensen K**, **Ingmer H**. 2005. Global virulence regulation in
725 *Staphylococcus aureus*: pinpointing the roles of ClpP and ClpX in the sar/agr regulatory
726 network. Infect Immun **73**:8100–8108.

727 16. **Jelsbak L**, **Ingmer H**, **Valihrach L**, **Cohn MT**, **Christiansen MHG**, **Kallipolitis BH**,
728 **Frees D**. 2010. The chaperone ClpX stimulates expression of *Staphylococcus aureus*
729 protein A by Rot dependent and independent pathways. PLoS ONE **5**:e12752.

730 17. **Kullik I**, **Giachino P**, **Fuchs T**. 1998. Deletion of the alternative sigma factor
731 sigmaB in *Staphylococcus aureus* reveals its function as a global regulator of virulence
732 genes. J Bacteriol **180**:4814–4820.

733 18. **Lu D**, **Wörmann ME**, **Zhang X**, **Schneewind O**, **Gründling A**, **Freemont PS**. 2009.
734 Structure-based mechanism of lipoteichoic acid synthesis by *Staphylococcus aureus*
735 LtaS. Proc Natl Acad Sci USA **106**:1584–1589.

736 19. **Bæk K**, **Gründling A**, **Mogensen RG**, **Thøgersen L**, **Petersen A**, **Paulander W**,
737 **Frees D**. 2014. β-Lactam resistance in methicillin-resistant *Staphylococcus aureus*
738 USA300 is increased by inactivation of the ClpXP protease. Antimicrob Agents
739 Chemother **58**:4593–4603.

740 20. **Zoll S**, **Schlag M**, **Shkumatov AV**, **Rautenberg M**, **Svergun DI**, **Götz F**, **Stehle T**.
741 2012. Ligand-binding properties and conformational dynamics of autolysin repeat
742 domains in staphylococcal cell wall recognition. J Bacteriol **194**:3789–3802.

743 21. **Feng J**, **Michalik S**, **Varming AN**, **Andersen JH**, **Albrecht D**, **Jelsbak L**, **Krieger**
744 **S**, **Ohlsen K**, **Hecker M**, **Gerth U**, **Ingmer H**, **Frees D**. 2013. Trapping and proteomic
745 identification of cellular substrates of the ClpP protease in *Staphylococcus aureus*. J
746 Proteome Res **12**:547–558.

747 22. **Pasquina LW**, **Santa Maria JP**, **Walker S**. 2013. Teichoic acid biosynthesis as an
748 antibiotic target. Curr Opin Microbiol **16**:531–537.

749 23. **Meredith TC**, **Wang H**, **Beaulieu P**, **Gründling A**, **Roemer T**. 2012. Harnessing the
750 power of transposon mutagenesis for antibacterial target identification and evaluation.
751 Mob Genet Elements **2**:171–178.

752 24. **Lutkenhaus J**, **Pichoff S**, **Du S**. 2012. Bacterial cytokinesis: From Z ring to
753 divisome. Cytoskeleton (Hoboken) **69**:778–790.

754 25. **Weart RB**, **Nakano S**, **Lane BE**, **Zuber P**, **Levin PA**. 2005. The ClpX chaperone
755 modulates assembly of the tubulin-like protein FtsZ. Mol Microbiol **57**:238–249.

756 26. **Dziedzic R**, **Kiran M**, **Plocinski P**, **Ziolkiewicz M**, **Brzostek A**, **Moomey M**,
757 **Vadrevu IS**, **Dziadek J**, **Madiraju M**, **Rajagopalan M**. 2010. Mycobacterium
758 tuberculosis ClpX Interacts with FtsZ and Interferes with FtsZ Assembly. PLoS ONE
759 **5**:e11058.

760 27. **Sugimoto S**, **Yamanaka K**, **Nishikori S**, **Miyagi A**, **Ando T**, **Ogura T**. 2010. AAA+
761 chaperone ClpX regulates dynamics of prokaryotic cytoskeletal protein FtsZ. J Biol
762 Chem **285**:6648–6657.

763 28. **Santa Maria JP**, **Sadaka A**, **Moussa SH**, **Brown S**, **Zhang YJ**, **Rubin EJ**, **Gilmore**
764 **MS**, **Walker S**. 2014. Compound-gene interaction mapping reveals distinct roles for
765 *Staphylococcus aureus* teichoic acids. Proc Natl Acad Sci USA **111**:12510–12515.

766 29. **R Core Team**. 2014. R: A language and environment for statistical computing. R
767 Foundation for Statistical Computing, Vienna, Austria.

768 30. **Zwietering MH**, **Jongenburger I**, **Rombouts FM**, **Riet K van 't**. 1990. Modeling of
769 the bacterial growth curve. Appl Environ Microbiol **56**:1875–1881.

770 31. **Giraud C**, **Hausmann S**, **Lemeille S**, **Prados J**, **Redder P**, **Linder P**. 2015. The C-
771 terminal region of the RNA helicase CshA is required for the interaction with the
772 degradosome and turnover of bulk RNA in the opportunistic pathogen *Staphylococcus*
773 *aureus*. RNA Biol **12**:658–674.

774 32. **Langmead B**, **Salzberg SL**. 2012. Fast gapped-read alignment with Bowtie 2. Nat
775 Methods **9**:357–359.

776 33. **Li H**, **Handsaker B**, **Wysoker A**, **Fennell T**, **Ruan J**, **Homer N**, **Marth G**, **Abecasis**
777 **G**, **Durbin R**, **1000 Genome Project Data Processing Subgroup**. 2009. The
778 Sequence Alignment/Map format and SAMtools. Bioinformatics **25**:2078–2079.

779 34. **Quinlan AR**, **Hall IM**. 2010. BEDTools: a flexible suite of utilities for comparing
780 genomic features. Bioinformatics **26**:841–842.

781 35. **Aziz RK**, **Bartels D**, **Best AA**, **DeJongh M**, **Disz T**, **Edwards RA**, **Formsma K**,
782 **Gerdes S**, **Glass EM**, **Kubal M**, **Meyer F**, **Olsen GJ**, **Olson R**, **Osterman AL**,
783 **Overbeek RA**, **McNeil LK**, **Paarmann D**, **Paczian T**, **Parrello B**, **Pusch GD**, **Reich C**,
784 **Stevens R**, **Vassieva O**, **Vonstein V**, **Wilke A**, **Zagnitko O**. 2008. The RAST Server:
785 rapid annotations using subsystems technology. BMC Genomics **9**:75.

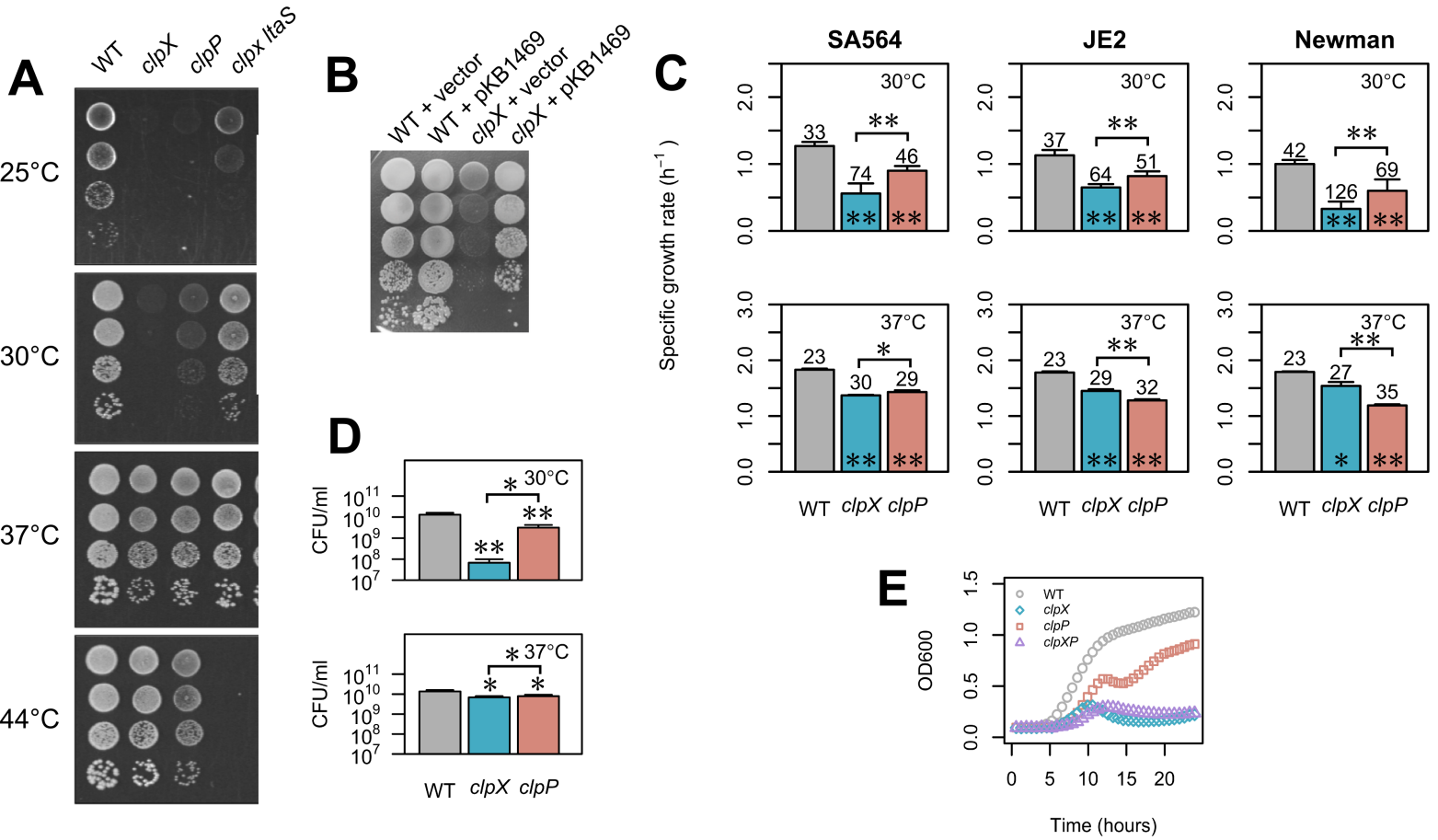
A
WT
clpX
clpP
clpx ltaS
25°C
30°C
37°C
44°C
B
WT + vector
WT + pKB1469
clpX + vector
clpX + pKB1469
C
SA564
JE2
Newman
Specific growth rate (h^{-1})
30°C
37°C
33
74
46
37
64
51
42
126
69
23
30
29
29
32
27
35
WT
clpX
clpP
D
CFU/ml
30°C
37°C
WT
clpX
clpP
E
OD600
WT
clpX
clpP
clpXP
Time (hours)

A

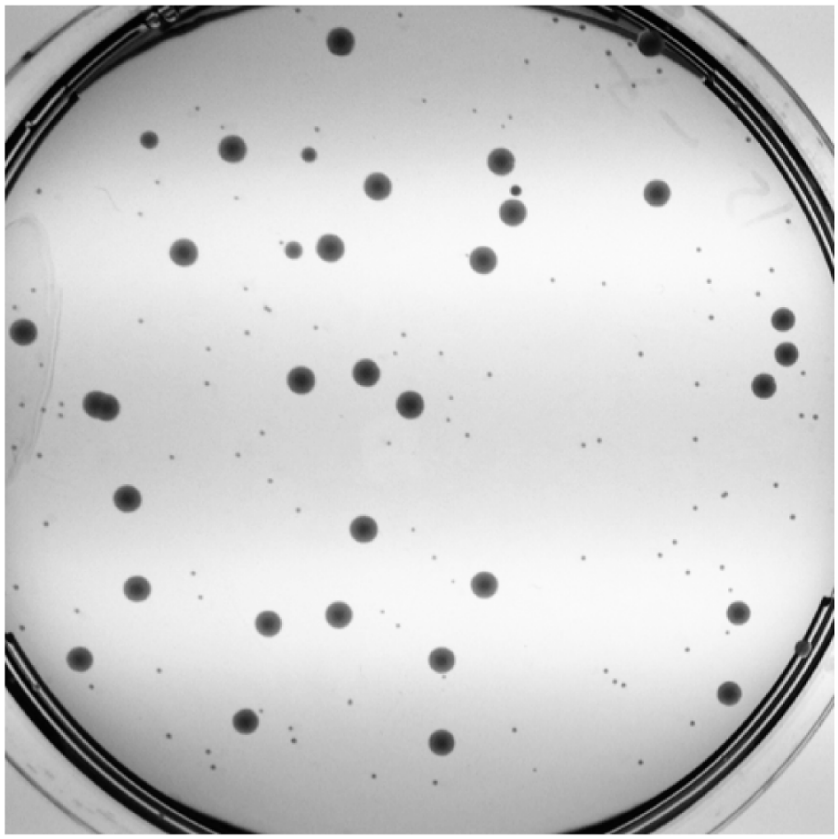

B

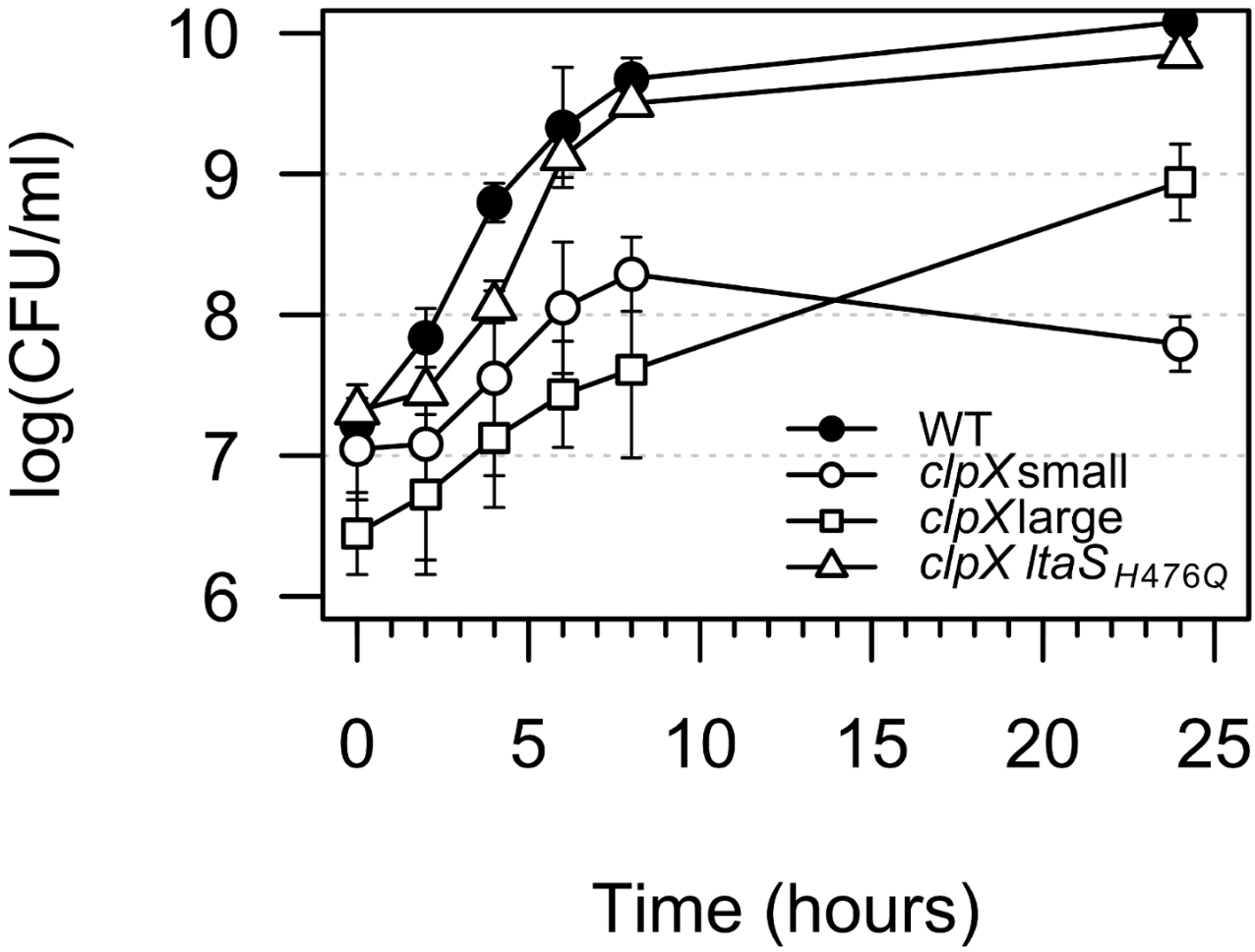
10
9
8
7
6
log(CFU/ml)
0
5
10
15
20
25
Time (hours)
WT
clpXsmall
clpXlarge
clpX ltaS H476Q

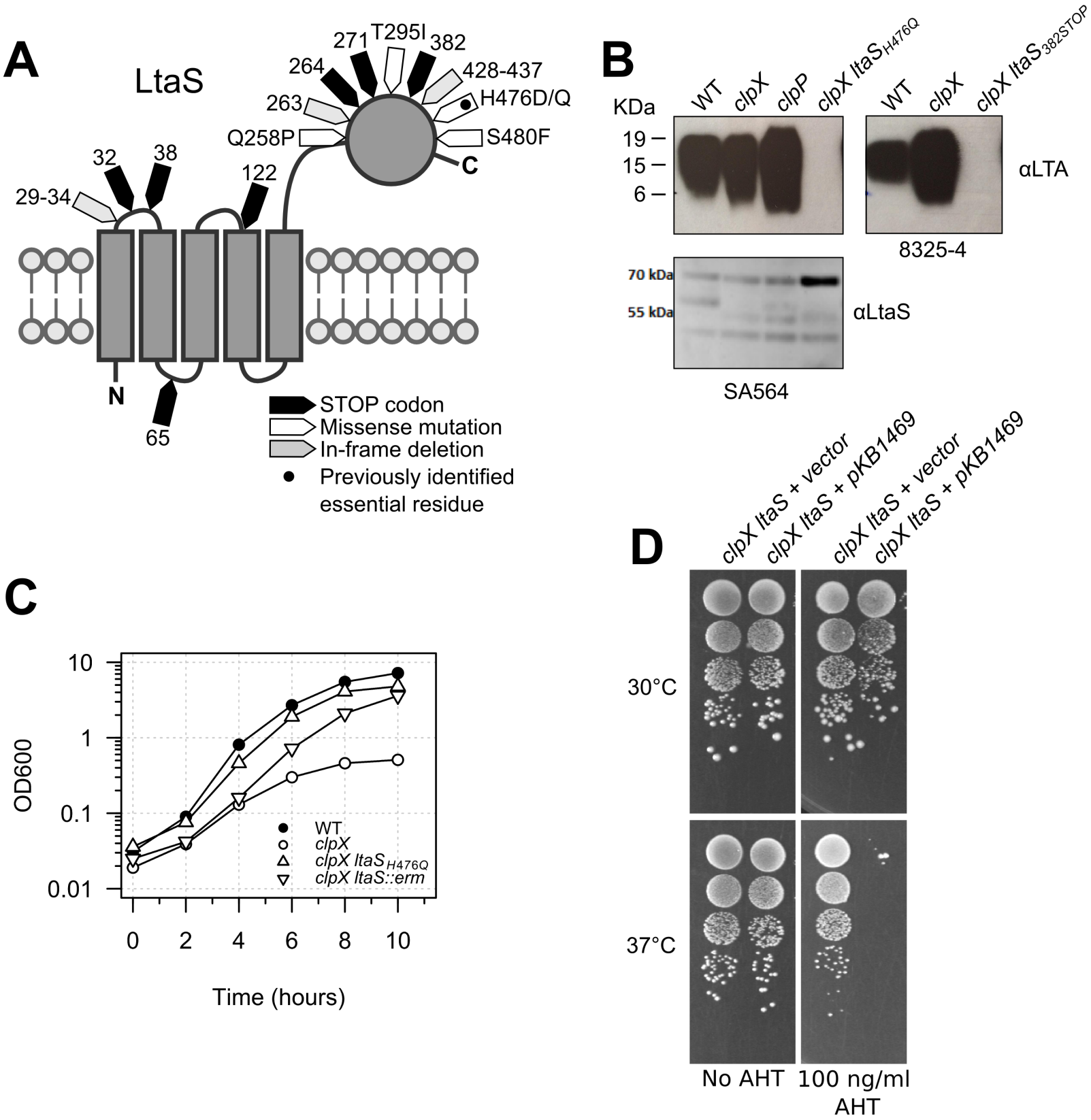
A
LtaS
271
T295I
382
264
428-437
263
H476D/Q
Q258P
S480F
C
32
38
122
29-34
N
65
STOP codon
Missense mutation
In-frame deletion
Previously identified essential residue
B
KDa
WT
clpX
clpP
clpX ltaS H476Q
WT
clpX
clpX ltaS 382STOP
19
15
6
αLTA
8325-4
70 kDa
55 kDa
αLtaS
SA564
C
OD600
10
1
0.1
0.01
0
2
4
6
8
10
Time (hours)
WT
clpX
clpX ltaS H476Q
clpX ltaS::erm
D
clpX ltaS + vector
clpX ltaS + pKB1469
clpX ltaS + vector
clpX ltaS + pKB1469
30°C
37°C
No AHT
100 ng/ml AHT

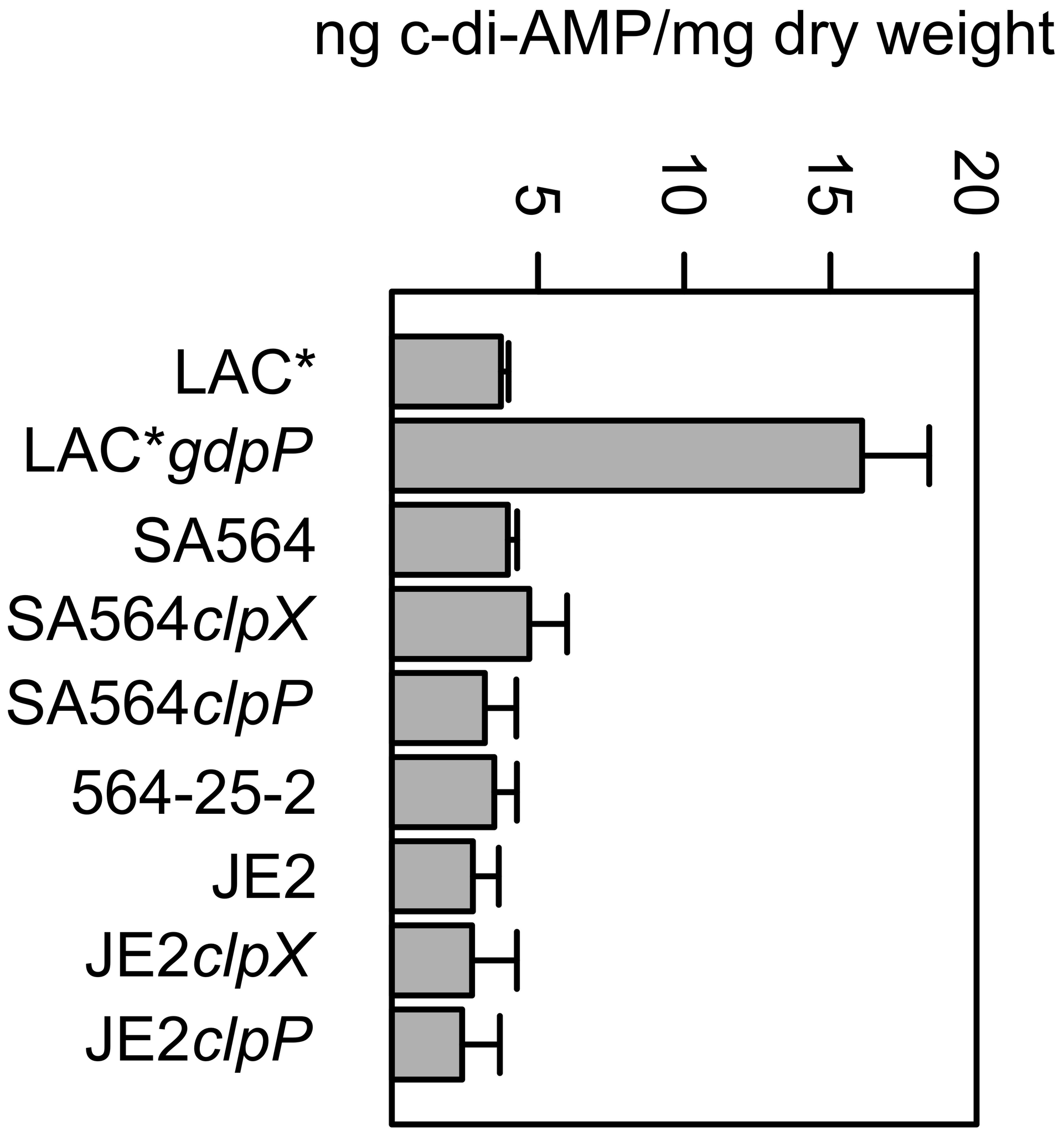
ng c-di-AMP/mg dry weight
5
10
15
20
LAC*
LAC*gdpP
SA564
SA564clpX
SA564clpP
564-25-2
JE2
JE2clpX
JE2clpP

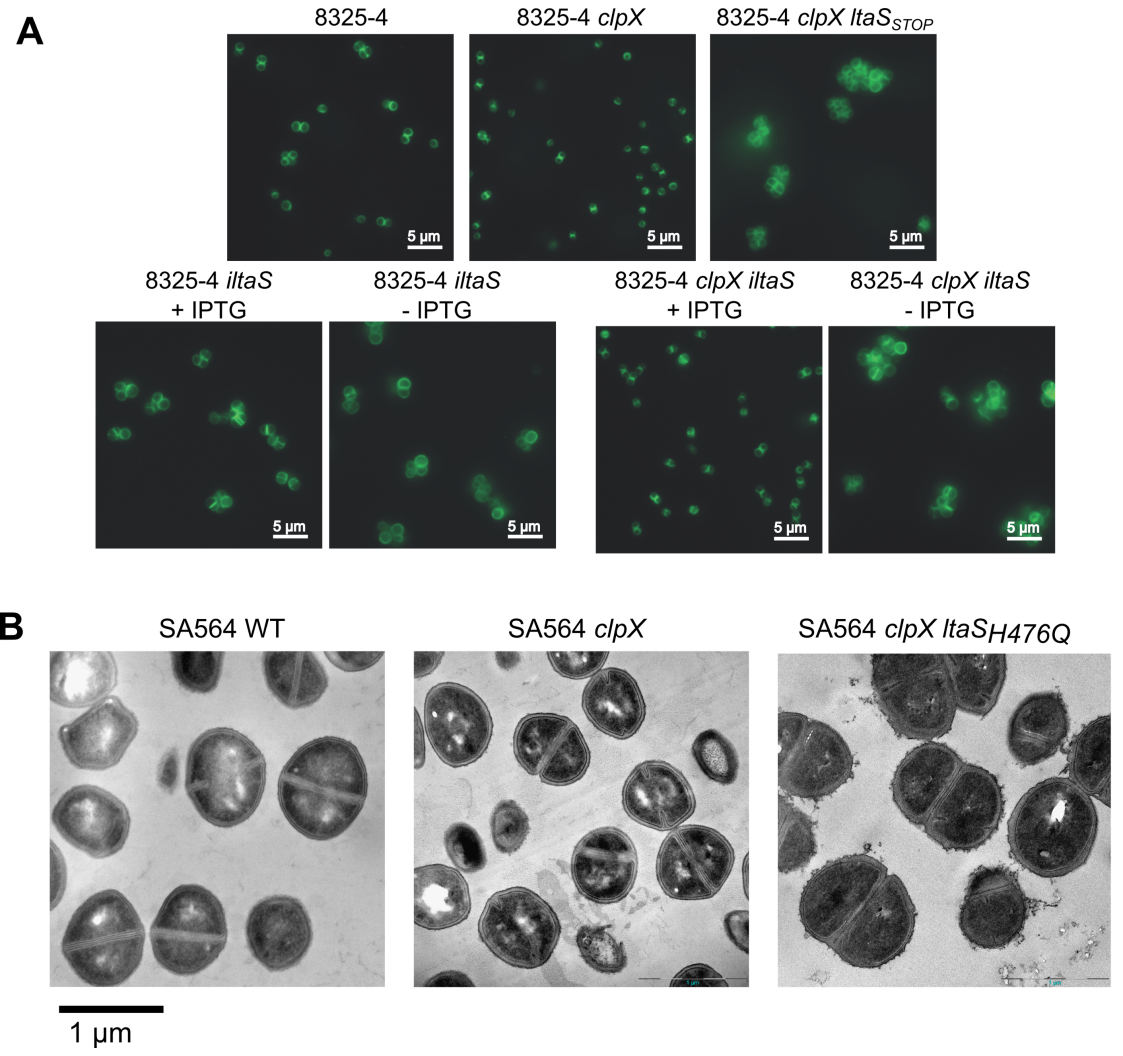
A
8325-4
8325-4 clpX
8325-4 clpX ltaS$_{STOP}$
5 µm
8325-4 iltaS + IPTG
8325-4 iltaS - IPTG
8325-4 clpX iltaS + IPTG
8325-4 clpX iltaS - IPTG
B
SA564 WT
SA564 clpX
SA564 clpX ltaS$_{H476Q}$
1 µm
C
Wild type
8%
12%
41%
39%
clpX
7%
11%
40%
42%
clpX-ltaS
11%
18%
49%
22%
Absorbance
Monomers
Dimers
Trimer - 8-mer
Higher oligomers

A

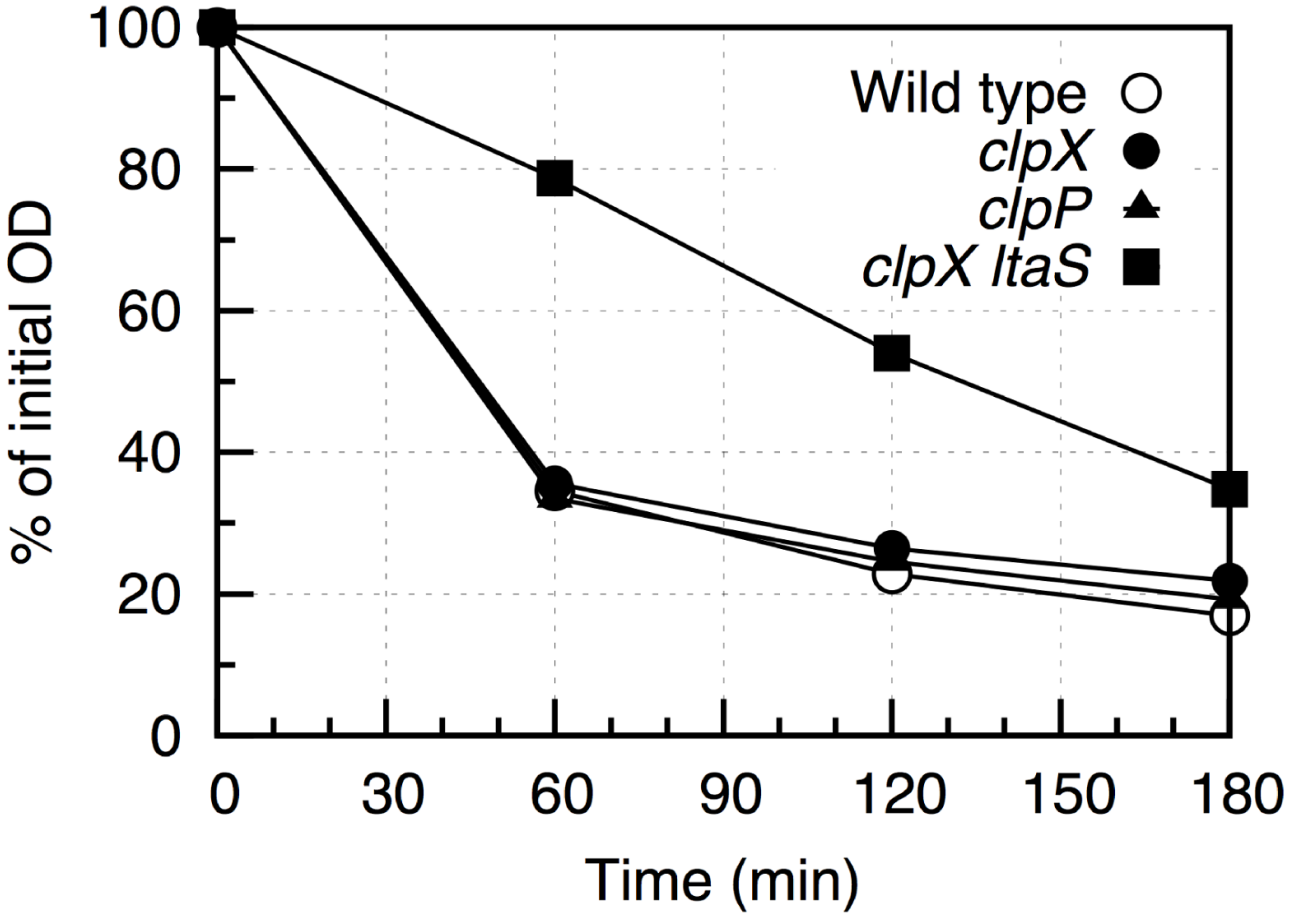
100
80
60
40
20
0
% of initial OD
0
30
60
90
120
150
180
Time (min)
Wild type
clpX
clpP
clpX ltaS

B

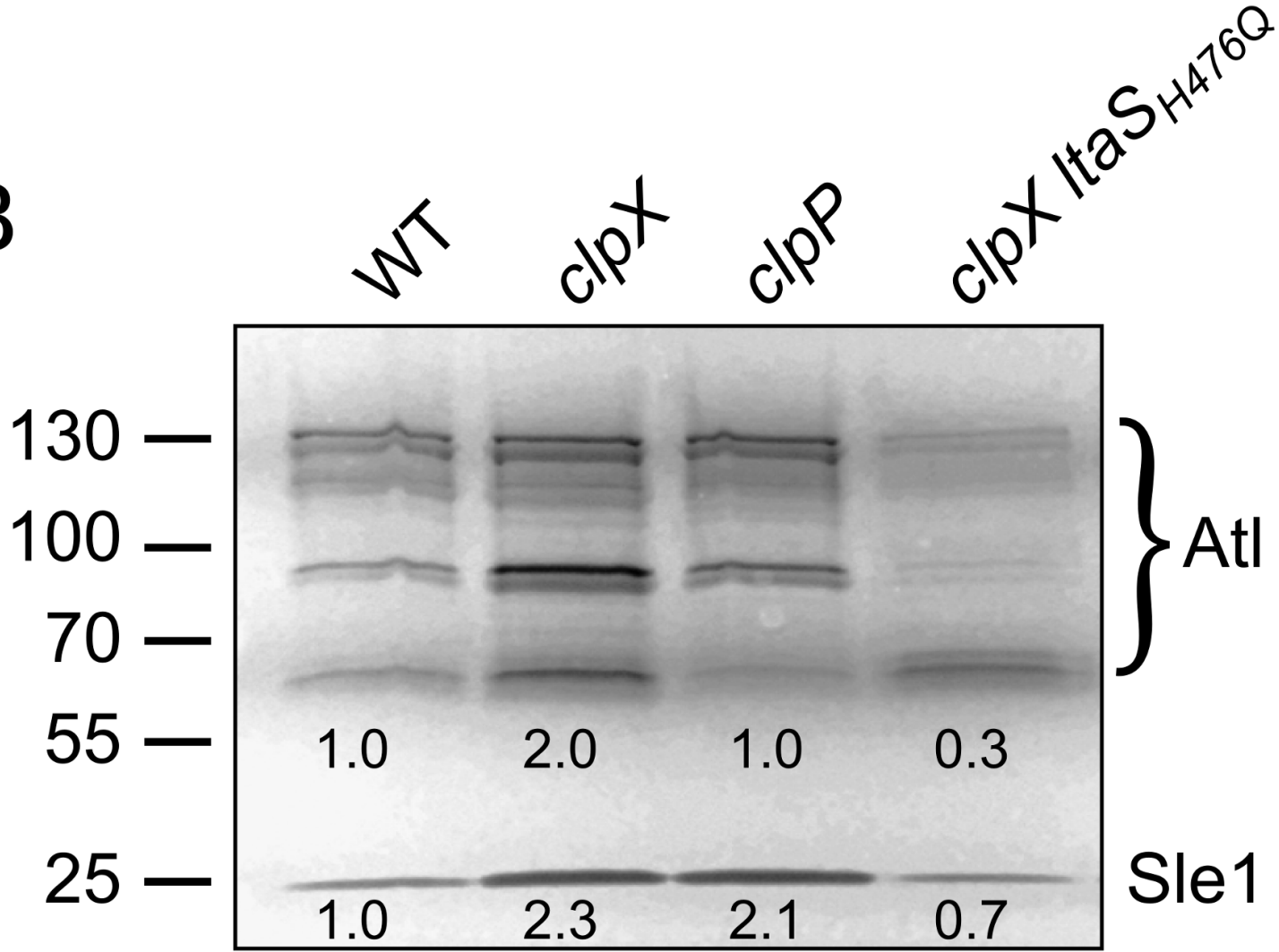
WT
clpX
clpP
clpX ltaS H476Q
130
100
70
55
25
Atl
Sle1
1.0
2.0
1.0
0.3
1.0
2.3
2.1
0.7